Fluorescent Mesostructured Polythiophene–Silica Composite Particles Synthesized by in Situ Polymerization of Structure-Directing Monomers

Zhi Yang, Xiaoshan Kou, Weihai Ni, Zhenhua Sun, Li Li, and Jianfang Wang*

Department of Physics, The Chinese University of Hong Kong, Shatin, Hong Kong SAR, P. R. China

Received July 25, 2007. Revised Manuscript Received September 27, 2007

Strongly fluorescent micrometer-sized mesostructured polythiophene–silica composite particles were synthesized, and their absorption and fluorescence properties were found to be dependent on their mesostructures. Two cationic trimethylammonium bromide surfactants carrying a thiophene group at the end of their hydrophobic tail were prepared to serve as both structure-directing agents and monomers. The synthesis using the surfactant with a 10-carbon chain in between the thiophene group and the positively charged headgroup under acidic conditions produced spherical particles with a wormlike mesostructure, and that using the surfactant with a 12-carbon chain yielded particles with curved morphologies and a two-dimensional hexagonal mesostructure. In situ polymerization of the thiophene groups closely packed in the central region of the nanoscale silica pore channels resulted in mesostructured polythiophene–silica composite particles. The absorption and fluorescence emission of the composite particles directed by the longer tail surfactant were found to be red-shifted relative to those of the particles directed by the shorter tail surfactant. This red shift was ascribed to the larger effective conjugation length of the polythiophene chains confined in the pore channels of the hexagonal mesostructure compared to that in the pore channels of the wormlike mesostructure.

Introduction

Control of the orientations of conjugated polymer chains is vital for the development of high-performance plastic electronic and optoelectronic devices. Polymers are wormlike in nature. When dispersed into matrices at dilute concentrations, conjugated polymers exhibit various conformations, such as defect cylinders and coils.[1] The collapse of a single conjugated chain leads to breaks in the π conjugation and π–π interactions between different segments of the chain. The breaks in the π conjugation result in a wide range of effective conjugation lengths. Since the excitation energy is strongly dependent on the effective conjugation length, the polymer chain exhibits an inhomogeneous distribution of photophysical properties such as the absorption and fluorescence emission energy. The π–π interactions provide shortened pathways for energy transfer. When processed into thin films from solutions for device fabrication, conjugated polymers typically form disordered structures with random orientations of chains in a wide variety of conformations. The coiled nature of polymer chains and their entanglement generate a large number of new pathways for energy transfer through π–π interactions between different chains. This three-dimensional energy transfer in solid polymer films usually leads to unidirectional energy migration to lower energy and nonemissive sites. It is therefore critical to be able to direct the orientations, conformations, and interactions of polymer chains in order to control the flow of excitations across conjugated polymer materials and reduce fluorescence quenching induced by energy transfer to defect sites. In the case of photovoltaic devices, efficient light harvesting and charge separation usually require the control of excitation energy transfer toward exciton dissociation regions, such as the interfaces in blends made of different materials.

Surfactant-templated mesoporous materials are attractive as hosts for the control of the orientations of conjugated polymers due to both their porous attributes and their simple solution-phase self-assembly process.[2] Their pores are tunable in size from 2 to 20 nm, and their pore organizations can vary among lamellar, two-/three-dimensional hexagonal, and cubic structures. Moreover, mesoporous silica used as hosts can protect conjugated polymers from photoinduced oxidation and decomposition and, at the same time, allow their optical properties to be probed from outside because silica is chemically stable, inert, and optically transparent. Three major methods have been developed for the incorporation of polymer chains into mesoporous channels. The first is the filling of mesopores with monomers, which are subsequently polymerized inside. Polymerizing catalysts are either supplied together with monomers or pregrafted/impregnated onto the inner walls of mesopores. Polyaniline, polyethylene, polyalkyne, poly(phenylene butadiynylene), polystyrene, and polymethacrylate have been prepared within

* To whom correspondence should be addressed. E-mail: jfwang@phy.cuhk.edu.hk.

(1) (a) Vanden Bout, D. A.; Yip, W.-T.; Hu, D. H.; Fu, D.-K.; Swager, T. M.; Barbara, P. F. *Science* **1997**, *277*, 1074. (b) Yu, J.; Hu, D. H.; Barbara, P. F. *Science* **2000**, *289*, 1327.

(2) (a) Soler-Illia, G. J. de A. A.; Sanchez, C.; Lebeau, B.; Patarin, J. *Chem. Rev.* **2002**, *102*, 4093. (b) Wan, Y.; Zhao, D. Y. *Chem. Rev.* **2007**, *107*, 2821.

10.1021/cm7020005 CCC: $37.00
Published on Web 11/10/2007

the channels of mesoporous silica using this method.[3] The resulting organic–inorganic composite materials exhibit interesting mechanical, optical, and electronic properties. In order for this method to be successful, mesopores should be accessible from outside for the filling of monomers. The second is the direct incorporation of polymers into mesopores through thermal cycling. Poly(phenylene vinylene) and its derivatives have been successfully infiltrated into hexagonally arrayed mesoporous channels, and control of energy transfer in oriented conjugated polymer–mesoporous silica composites has been demonstrated.[4] This method requires mesoporous materials with highly ordered one-dimensional pore channels that are accessible from outside. In addition, because the infiltration of polymer chains into preformed mesoporous materials depends on their partitioning from solvents, it is expected to be difficult to control the concentration and uniformity of polymers in mesoporous materials. Further, when the pore size is smaller than the radius of gyration of solvated polymer chains, infiltration by threading polymer chains through the pore usually requires rather long processing times at elevated temperatures. The third method is the design of special amphiphilic molecules that can serve as both structure-directing agents and monomers. This method has so far mainly been applied to molecules containing diacetylene groups.[5] The resulting polydiacetylene–silica composites are optically transparent and mechanically robust. They exhibit interesting thermo-, solvato-, and mechanochromic properties. In addition, pyrrole-containing cationic ammonium surfactants have also been recently synthesized and used as structure-directing agents to prepare polypyrrole–silica composite thin films through spin-coating.[6]

In this work we exploit the hybrid organic–inorganic self-assembly approach to prepare mesostructured polythiophene–silica composite particles under strongly acidic aqueous solutions. We focus on conjugated polythiophenes because polythiophenes and their derivatives exhibit relatively high charge mobilities ($0.2-0.6\ cm^2\ V^{-1}\ s^{-1}$)[7] when compared to other conjugated polymers. They have been widely used as active materials for fabricating electronic and optoelectronic devices, including thin-film field-effect transistors[8] and plastic photovoltaic cells.[9] In addition, thiophene monomers can be readily polymerized through catalytic reactions.[10] Two cationic ammonium surfactants that have different hydrophobic tail lengths and contain a thiophene group at the end of their tail are first synthesized and then used as both structure-directing agents and monomers. The self-assembly process locks both organic and inorganic precursors into three-dimensional arrangements. In situ polymerization produces conjugated polythiophenes that are uniformly distributed within an inorganic environment. In contrast with postloading approaches,[3,4] the self-assembly method guarantees a dense and intimate filling of conjugated polymers into mesoporous silica channels.

The assembly of organic and inorganic precursors under acidic conditions allows for the production of mesostructured silica materials with well-controlled internal architectures and morphologies,[11] such as spheres,[12] gyroids,[13] fibers,[14–16] and ribbons.[17] The use of our synthesized thiophene-containing cationic surfactants with two different tail lengths results in micrometer-sized polythiophene–silica composite spheres and gyroidal particles with distinct internal mesostructures. In comparison, the assembly using similar thiophene-containing surfactants under basic conditions has been reported previously, with major efforts focused on the gram-scale synthesis of submicrometer-long polythiophenes through the assembly process.[18] Our mesostructured polythiophene–silica com-

(3) (a) Wu, C.-G.; Bein, T. *Science* **1994**, *264*, 1757. (b) Kageyama, K.; Tamazawa, J.-I.; Aida, T. *Science* **1999**, *285*, 2113. (c) Cardin, D. J.; Constantine, S. P.; Gilbert, A.; Lay, A. K.; Alvaro, M.; Galletero, M. S.; Garcia, H.; Marquez, F. *J. Am. Chem. Soc.* **2001**, *123*, 3141. (d) Lin, V. S.-Y.; Radu, D. R.; Han, M.-K.; Deng, W. H.; Kuroki, S.; Shanks, B. H.; Pruski, M. *J. Am. Chem. Soc.* **2002**, *124*, 9040. (e) Choi, M.; Kleitz, F.; Liu, D. N.; Lee, H. Y.; Ahn, W.-S.; Ryoo, R. *J. Am. Chem. Soc.* **2005**, *127*, 1924.

(4) (a) Wu, J. J.; Gross, A. F.; Tolbert, S. H. *J. Phys. Chem. B* **1999**, *103*, 2374. (b) Nguyen, T.-Q.; Wu, J. J.; Doan, V.; Schwartz, B. J.; Tolbert, S. H. *Science* **2000**, *288*, 652. (c) Tolbert, S. H.; Wu, J. J.; Gross, A. F.; Nguyen, T.-Q.; Schwartz, B. J. *Microporous Mesoporous Mater.* **2001**, *44–45*, 445. (d) Qi, D. F.; Kwong, K.; Rademacher, K.; Wolf, M. O.; Young, J. F. *Nano Lett.* **2003**, *3*, 1265. (e) Molenkamp, W. C.; Watanabe, M.; Miyata, H.; Tolbert, S. H. *J. Am. Chem. Soc.* **2004**, *126*, 4476.

(5) (a) Aida, T.; Tajima, K. *Angew. Chem., Int. Ed.* **2001**, *40*, 3803. (b) Lu, Y. F.; Yang, Y.; Sellinger, A.; Lu, M. C.; Huang, J. M.; Fan, H. Y.; Haddad, R.; Lopez, G.; Burns, A. R.; Sasaki, D. Y.; Shelnutt, J.; Brinker, C. J. *Nature (London)* **2001**, *410*, 913. (c) Yang, Y.; Lu, Y. F.; Lu, M. C.; Huang, J. M.; Haddad, R.; Xomeritakis, G.; Liu, N. G.; Malanoski, A. P.; Sturmayr, D.; Fan, H. Y.; Sasaki, D. Y.; Assink, R. A.; Shelnutt, J. A.; van Swol, F.; Lopez, G. P.; Burns, A. R.; Brinker, C. J. *J. Am. Chem. Soc.* **2003**, *125*, 1269. (d) Peng, H. S.; Tang, J.; Pang, J. B.; Chen, D. Y.; Yang, L.; Ashbaugh, H. S.; Brinker, C. J.; Yang, Z. Z.; Lu, Y. F. *J. Am. Chem. Soc.* **2005**, *127*, 12782. (e) Peng, H. S.; Tang, J.; Yang, L.; Pang, J. B.; Ashbaugh, H. S.; Brinker, C. J.; Yang, Z. Z.; Lu, Y. F. *J. Am. Chem. Soc.* **2006**, *128*, 5304.

(6) Ikegame, M.; Tajima, K.; Aida, T. *Angew. Chem., Int. Ed.* **2003**, *42*, 2154.

(7) McCulloch, I.; Heeney, M.; Bailey, C.; Genevicius, K.; MacDonald, I.; Shkunov, M.; Sparrowe, D.; Tierney, S.; Wagner, R.; Zhang, W. M.; Chabinyc, M. L.; Kline, R. J.; McGehee, M. D.; Toney, M. F. *Nat. Mater.* **2006**, *5*, 328.

(8) (a) Sirringhaus, H.; Brown, P. J.; Friend, R. H.; Nielsen, M. M.; Bechgaard, K.; Langeveld-Voss, B. M. W.; Spiering, A. J. H.; Janssen, R. A. J.; Meijer, E. W.; Herwig, P.; de Leeuw, D. M. *Nature (London)* **1999**, *401*, 685. (b) Stutzmann, N.; Friend, R. H.; Sirringhaus, H. *Science* **2003**, *299*, 1881.

(9) (a) Ma, W. L.; Yang, C. Y.; Gong, X.; Lee, K.; Heeger, A. J. *Adv. Funct. Mater.* **2005**, *15*, 1617. (b) Li, G.; Shrotriya, V.; Huang, J. S.; Yao, Y.; Moriarty, T.; Emery, K.; Yang, Y. *Nat. Mater.* **2005**, *4*, 864. (c) Kim, Y.; Cook, S.; Tuladhar, S. M.; Choulis, S. A.; Nelson, J.; Durrant, J. R.; Bradley, D. D. C.; Giles, M.; McCulloch, I.; Ha, C.-S.; Ree, M. *Nat. Mater.* **2006**, *5*, 197.

(10) McCullough, R. D. *Adv. Mater.* **1998**, *10*, 93.

(11) (a) Huo, Q. S.; Margolese, D. I.; Ciesla, U.; Feng, P. Y.; Gier, T. E.; Sieger, P.; Leon, R.; Petroff, P. M.; Schüth, F.; Stucky, G. D. *Nature (London)* **1994**, *368*, 317. (b) Huo, Q. S.; Margolese, D. I.; Ciesla, U.; Demuth, D. G.; Feng, P. Y.; Gier, T. E.; Sieger, P.; Firouzi, A.; Chmelka, B. F.; Schüth, F.; Stucky, G. D. *Chem. Mater.* **1994**, *6*, 1176.

(12) Yang, H.; Vovk, G.; Coombs, N.; Sokolov, I.; Ozin, G. A. *J. Mater. Chem.* **1998**, *8*, 743.

(13) (a) Yang, H.; Coombs, N.; Ozin, G. A. *Nature (London)* **1997**, *386*, 692. (b) Yang, H.; Ozin, G. A.; Kresge, C. T. *Adv. Mater.* **1998**, *10*, 883. (c) Yang, S. M.; Yang, H.; Coombs, N.; Sokolov, I.; Kresge, C. T.; Ozin, G. A. *Adv. Mater.* **1999**, *11*, 52.

(14) (a) Huo, Q. S.; Zhao, D. Y.; Feng, J. L.; Weston, K.; Buratto, S. K.; Stucky, G. D.; Schacht, S.; Schüth, F. *Adv. Mater.* **1997**, *9*, 974. (b) Marlow, F.; McGehee, M. D.; Zhao, D. Y.; Chmelka, B. F.; Stucky, G. D. *Adv. Mater.* **1999**, *11*, 632. (c) Loerke, J.; Marlow, F. *Adv. Mater.* **2002**, *14*, 1745.

(15) Wang, J. F.; Zhang, J. P.; Asoo, B. Y.; Stucky, G. D. *J. Am. Chem. Soc.* **2003**, *125*, 13966.

(16) Wang, J. F.; Tsung, C.-K.; Hong, W. B.; Wu, Y. Y.; Tang, J.; Stucky, G. D. *Chem. Mater.* **2004**, *16*, 5169.

(17) Wang, J. F.; Tsung, C.-K.; Hayward, R. C.; Wu, Y. Y.; Stucky, G. D. *Angew. Chem., Int. Ed.* **2005**, *44*, 332.

(18) Li, G. T.; Bhosale, S.; Wang, T. Y.; Zhang, Y.; Zhu, H. S.; Fuhrhop, J.-H. *Angew. Chem., Int. Ed.* **2003**, *42*, 3818.

posite particles emit bright, photostable fluorescence. Their absorption and fluorescence properties are found to be dependent on the hydrophobic tail length of the surfactants. Such fluorescent particles can be of particular use in a number of applications, including flow cytometry and the labeling of skin care products.[19]

Experimental Section

Materials and Instruments. All commercially available materials were used as received. 4-Methoxyphenol, 1,10-dibromodecane, 1,12-dibromododecane, magnesium turnings, 3-bromothiophene, [1,3-bis(diphenylphosphino)propane]dichloronickle(II) ($NiDPPPCl_2$), acetic anhydride, and tetraethyl orthosilicate (TEOS) were purchased from Aldrich. Anhydrous iron(III) chloride was obtained from Merck. Hydrobromic acid (48 wt %) and trimethylamine (33 wt % in ethanol) were obtained from Acros. Nuclear magnetic resonance (NMR) spectra were recorded with a Bruker DPX-300 spectrometer (300.13 MHz for ^1H NMR and 75.47 MHz for ^{13}C NMR). All NMR measurements were carried out at room temperature in deuterated chloroform solutions. Chemical shifts (δ) are reported in parts per million (ppm). Mass spectra (EI-MS and ESI-MS) were measured using a Thermo Finnigan MAT95XL mass spectrometer. Scanning electron microscopy (SEM) imaging was performed on a FEI Quanta 400 FEG microscope. Transmission electron microscopy (TEM) imaging was performed on a FEI CM120 microscope at 120 kV. Samples for TEM characterization were calcined at 500 °C for 5 h in air with a heating rate of 1 °C/min, ground gently, dispersed in ethanol by ultrasonication, and then deposited on TEM copper grids that are coated with lacey Formvar and stabilized with carbon. Small-angle X-ray diffraction (SAXRD) patterns were obtained on a Bruker D8 Advance X-ray diffractometer with Cu Kα radiation. UV–vis absorption spectra were acquired using a Hitachi U-3501 spectrophotometer. Fluorescence emission and excitation spectra were acquired using a Hitachi F-4500 spectrofluorometer. Samples for absorption and fluorescence spectral measurements were dispersed in deionized water at a concentration of 0.25 wt %. A custom-built optical system was used for fluorescence imaging and spectroscopy measurements on individual mesostructured polythiophene–silica composite particles. Particles deposited on glass slides were excited with the 457 nm laser line from a Spectra-Physics Stabilite 2017 argon ion laser. The excitation light was reflected from a dichroic mirror and focused by an Olympus 50× objective with a numerical aperture of 0.75. The excitation power density was ~1 kW/cm^2. Fluorescence was collected by the same objective, passed through a long-pass filter with a 50% cutoff wavelength at 530 nm to remove the excitation light, focused onto the entrance slit of an Acton SpectraPro 2300i spectrometer, and either imaged or spectrally dispersed onto a Princeton Instruments Pixis 512 charge coupled device (CCD) that was thermoelectrically cooled to −50 °C. The exposure time was typically set at 10 s.

10-(*p*-Methoxyphenoxy)decyl Bromide and 12-(*p*-Methoxyphenoxy)dodecyl Bromide. Potassium hydroxide (13.5 g, 0.24 mol) in 200 mL of methanol was mixed with 4-methoxyphenol (24.8 g, 0.2 mol) in 100 mL of methanol. The resulting solution was added within 1.5 h to 1,10-dibromodecane (120 g, 0.4 mol) or 1,12-dibromododecane (131.2 g, 0.4 mol) in 400 mL of acetone. The mixture was refluxed for 5 h, concentrated, and diluted with water. The oil phase was transferred in diethyl ether. The ether extract was then filtered, washed with dilute sodium hydroxide and water, dried, condensed, and recrystallized from hexane, giving 10-(*p*-methoxyphenoxy)decyl bromide (53.5 g) or 12-(*p*-methoxyphenoxy)dodecyl bromide (59.4 g). The yield relative to the used amount of 4-methoxyphenol is ~80%.

3-[10-(*p*-Methoxyphenoxy)decyl]thiophene and 3-[12-(*p*-Methoxyphenoxy)dodecyl]thiophene. 10-(*p*-methoxyphenoxy)decyl bromide (42.88 g, 0.125 mol) or 12-(*p*-methoxyphenoxy)dodecyl bromide (46.38 g, 0.125 mol) in 40 mL of anhydrous diethyl ether was added under an inert atmosphere to magnesium turnings (3.16 g, 0.13 mol) in 10 mL of anhydrous diethyl ether. The reaction mixture was refluxed for 5 h. The Grignard compound solution was subsequently transferred via a cannula to a second apparatus and added dropwise at 0 °C to $NiDPPPCl_2$ (70 mg, 0.13 mmol) and 3-bromothiophene (17.2 g, 0.106 mol) over 1 h. The reaction mixture was refluxed for 15 h and afterward hydrolyzed with 40 mL of HCl (1.0 M) and 150 mL of ice–water, followed by extraction with several portions of diethyl ether. Washing to neutrality, drying of the combined organic phases, and removal of the solvent in vacuum gave a white solid, which was recrystallized from methanol to produce analytically pure 3-[10-(*p*-methoxyphenoxy)decyl]thiophene (31.6 g) or 3-[12-(*p*-methoxyphenoxy)dodecyl]thiophene (35.5 g) in ~75% yield.

3-(10-Bromodecyl)thiophene and 3-(12-Bromododecyl)thiophene. A mixture of HBr (20.2 g, 48 wt %, 0.12 mol) and acetic anhydride (20.2 g, 0.198 mol) was added under inert atmosphere to 3-[10-(*p*-methoxyphenoxy)decyl]thiophene (6.92 g, 0.02 mol) or 3-[12-(*p*-methoxyphenoxy)dodecyl]thiophene (7.48 g, 0.02 mol), and the reaction mixture was refluxed for 30 h. After dilution with water, the mixture was extracted several times with diethyl ether, and the combined organic phase was washed to neutrality with saturated $NaHCO_3$ solution. Drying of the organic phase and removal of the solvent gave a yellow-brown oil, from which hydroquinone was precipitated by the addition of a mixture of hexane and diethyl ether. The solution was then filtered, transferred to a short silica gel column, and eluted with hexane. Removal of the solvent gave a colorless and analytically pure oil of 3-(10-bromodecyl)thiophene (4.79 g) or 3-(12-bromododecyl)thiophene (5.30 g) in ~80% yield. 3-(10-Bromodecyl)thiophene: ^1H NMR ($CDCl_3$): δ 7.15 (dd, 1 H, J = 3, 4.8 Hz), 6.85 (d, 1 H, J = 5.1 Hz), 6.83 (d, 1 H, J = 3.9 Hz), 3.34 (t, 2 H, J = 6.8 Hz), 2.54 (t, 2 H, J = 7.6 Hz), 1.77 (m, 2 H), 1.54 (m, 2 H), 1.26 (s, 12 H); ^{13}C NMR ($CDCl_3$): δ 143.12, 128.21, 124.99, 119.71, 34.02, 32.77, 30.50, 30.22, 29.37, 29.25, 28.70, 28.11; MS (EI): m/z = 302 (M^+), 223 ($C_{14}H_{23}S^+$), 98 ($C_5H_6S^+$). 3-(12-Bromododecyl)thiophene: ^1H NMR ($CDCl_3$): δ 7.23 (dd, 1 H, J = 2.8, 4.5 Hz), 6.92 (d, 1 H, J = 5.4 Hz), 6.90 (d, 1 H, J = 0.9 Hz), 3.40 (t, 2 H, J = 6.9 Hz), 2.61 (t, 2 H, J = 7.8 Hz), 1.85 (m, 2 H), 1.61 (m, 2 H), 1.27 (s, 16 H); ^{13}C NMR ($CDCl_3$): δ 143.18, 128.23, 124.98, 119.70, 34.02, 32.80, 30.53, 30.24, 29.54, 29.43, 29.30, 28.73, 28.14; MS (EI): m/z = 330 (M^+), 251 ($C_{16}H_{27}S^+$), 98 ($C_5H_6S^+$).

Trimethyl-(10-thiophen-3-yl-decyl)ammonium Bromide (TC10TMA) and Trimethyl-(12-thiophen-3-yl-dodecyl)ammonium Bromide (TC12TMA). TC10TMA and TC12TMA were prepared by mixing 3-(10-bromodecyl)thiophene (4.54 g, 0.015 mol) and 3-(12-bromododecyl)thiophene (4.96 g, 0.015 mol), respectively, with a 30% excess of trimethylamine in ethanol and then refluxing for 24 h. The mixture remaining after reflux was rotary-evaporated to remove the solvent. The resulting solid product was recrystallized from ethyl acetate to give TC10TMA (4.83 g) or TC12TMA (5.26 g) in ~90% yield. TC10TMA: MS (ESI): m/z = 282 $(C_{17}H_{32}NS)^+$. TC12TMA: MS (ESI): m/z = 310 $(C_{19}H_{36}NS)^+$.

Synthesis of Mesostructured TC10TMA–Silica and TC12TMA–Silica Composite Particles. The synthesis of mesostructured composite particles was started by mixing calculated amounts of the thiophene-containing cationic surfactants, distilled

(19) Iyer, S.; Kievsky, Y.; Sokolov, I. *Skin Res. Technol.* **2007**, *13*, 317.

Scheme 1. Synthesis of the Two Thiophene-Containing Cationic Surfactants TC10TMA and TC12TMA

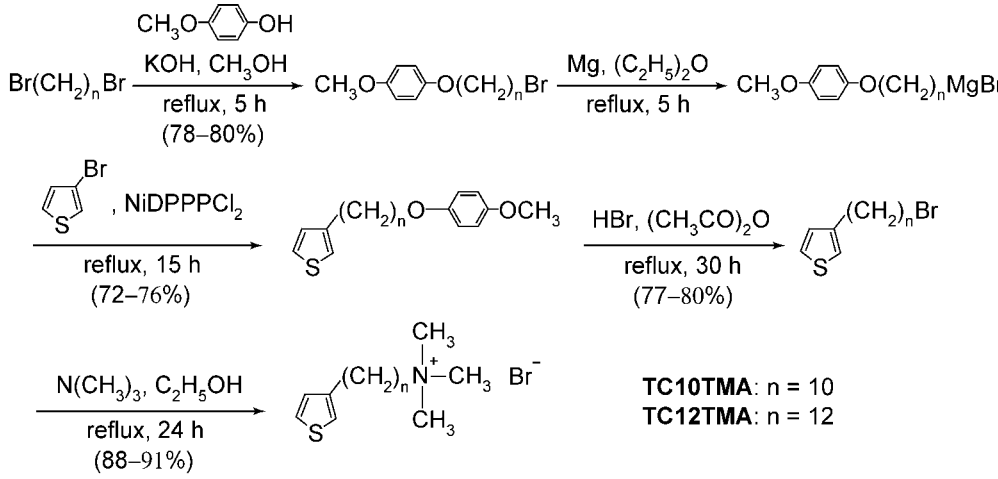

Scheme 2. Formation of Mesostructured Polythiophene–Silica Composite Particles through in Situ Polymerization

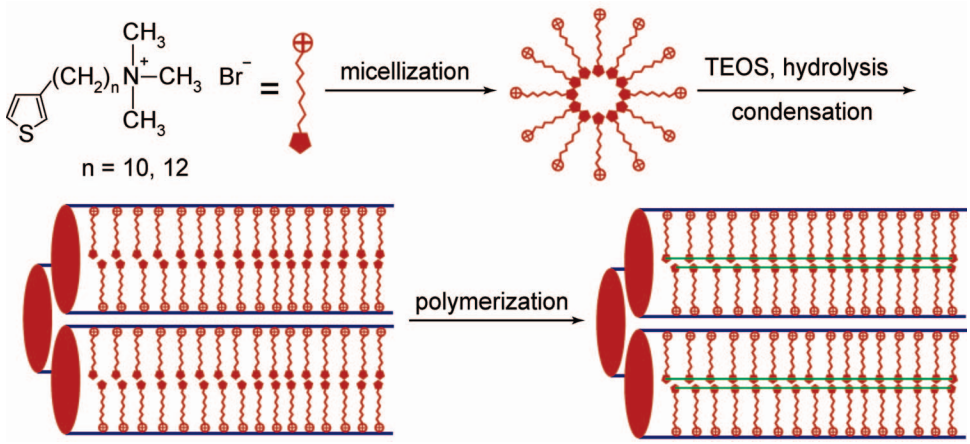

water, and concentrated HCl acid (37 wt %). The mixture was stirred until the surfactants were completely dissolved. The silica precursor, TEOS, was then added at a molar ratio of 100 H_2O/7 HCl/0.02 surfactant/0.03 TEOS. The resulting solution was stirred at room temperature for 10 min and then transferred to a glass bottle. The bottle was closed and kept in an isothermal oven at 65 °C for 48 h. During this period of time, particles were observed to form and precipitate at the bottom of the bottle. They were taken out, washed three times with water by centrifugation, and dried at 100 °C in air.

In Situ Polymerization of Thiophene Groups. Anhydrous iron(III) chloride (0.8 g) and dried chloroform (10 mL) were placed in a round-bottom flask under a flow of argon, and then mesostructured TC10TMA–silica or TC12TMA–silica composite particles (0.2 g) were added. The resulting mixture was stirred at room temperature for 48 h under continuously flowing argon. The particles after polymerization were washed three times with water by centrifugation and dried at 100 °C in air.

Results and Discussion

The synthesis of the two thiophene-containing cationic surfactants TC10TMA and TC12TMA was adapted from the previously reported procedure for the preparation of 3-(ω-haloalkyl)thiophenes with shorter alkyl chains.[20] The methodology is summarized in Scheme 1. The synthesis started with the reaction of 1,10-dibromodecane and 1,12-dibromododecane with 4-methoxyphenol to give 10-(*p*-methoxyphenoxy)decyl bromide and 12-(*p*-methoxyphenoxy)dodecyl bromide, respectively. The resulting ω-(*p*-methoxyphenoxy) alkyl bromides reacted readily with magnesium to give the corresponding Grignard compounds in nearly quantitative yields. The Grignard compounds were then coupled to 3-bromothiophene by refluxing in diethyl ether in the presence of $NiDPPPCl_2$ as a catalyst to form terminally protected 3-[ω-(*p*-methoxyphenoxy)alkyl]thiophenes. The 4-methoxyphenoxy protecting group was cleaved by refluxing in the presence of hydrobromic acid and acetic anhydride to yield 3-(ω-bromoalkyl)thiophenes. The cationic ammonium surfactants containing a thiophene group at the end of their hydrophobic tail was then obtained by the reaction of trimethylamine with 3-(ω-bromoalkyl)thiophenes in alcoholic solutions.[21]

The thiophene-containing surfactants TC10TMA and TC12TMA were used as structure-directing agents to prepare mesostructured composite particles in a one-phase route under strongly acidic conditions,[15–17] as shown schematically in Scheme 2. TEOS was used as the silica precursor. The molar ratio of the reaction mixture was established at 100

(20) Bäuerle, P.; Würthner, F.; Heid, S. *Angew. Chem., Int. Ed.* **1990**, *29*, 419.

(21) Scott, A. B.; Tartar, H. V. *J. Am. Chem. Soc.* **1943**, *65*, 692.

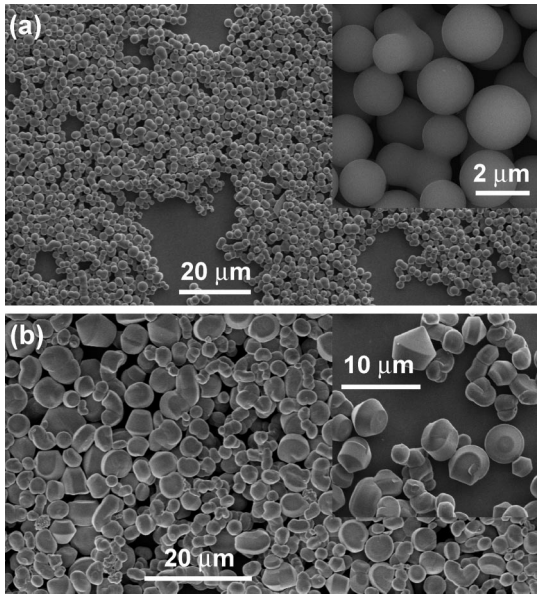

Figure 1. SEM images of as-prepared mesostructured silica particles. (a) Spherical particles prepared with TC10TMA. (b) Particles of curved morphologies prepared with TC12TMA. The insets are zoomed-in SEM images.

H_2O/7 HCl/0.02 surfactant/0.03 TEOS. During reaction, particles were observed to form and precipitate to the bottom of the container. These particles were washed and deposited onto silicon substrates for SEM observation. Parts a and b of Figure 1 show representative SEM images of the particles made with TC10TMA and TC12TMA, respectively. The particles made with TC10TMA are all spheres, some of which are agglomerated together. Their diameters are in the range 0.5−4 μm, with an average of 2.2 ± 0.4 μm. In contrast, the particles made with TC12TMA possess fascinating morphologies with diverse shapes and curvatures. Most particles are gyroidal, displaying faceted smooth surfaces that emanate radially or spirally from the topologically unique rotation axis. Their typical dimensions are in the range 2−7 μm. The curved surfaces are the manifestation of pore channels running along the circumference around the axis of symmetry of the particles. For comparison, alkyltrimethylammonium bromide surfactants of different hydrophobic tail lengths have previously been used as structure-directing agents to synthesize mesostructured silica materials under similar acidic conditions.[16] The morphology of the products varies from spheres through particles with curved morphologies to nanofibers as the surfactant tail length increases from a 12-carbon chain to an 18-carbon chain. When the surfactant tail is dodecyl, micrometer-sized spherical particles are obtained. When the surfactant tail becomes tetradecyl, micrometer-sized particles with curved morphologies are obtained. The synthesis with the surfactant of a hexadecyl tail produces both mesostructured nanofibers and particles with curved morphologies. Further, almost all the products obtained from the synthesis with the surfactant of an octadecyl tail are mesostructured nanofibers. The effective tail length of the two thiophene-containing trimethylammonium surfactants can therefore be approximately estimated on the basis of the morphologies of their mesostructured products. The hydrophobic tail of TC10TMA, which contains a 10-carbon chain and a thiophene group at the end of the chain, is roughly equivalent to a 12-carbon chain in templating the mesostructure formation, and that of TC12TMA is roughly equivalent to a 14-carbon chain in directing the formation of mesostructured silica materials.

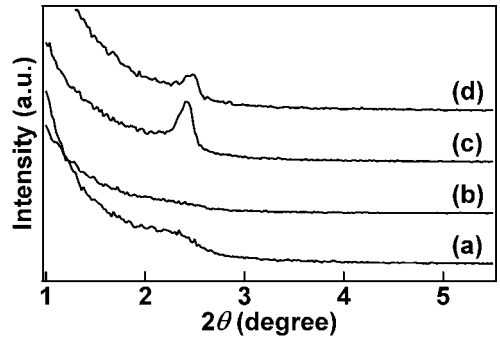

Figure 2. SAXRD patterns of mesostructured silica particles. (a) As-prepared particles containing TC10TMA. (b) Particles containing polymerized TC10TMA. (c) As-prepared particles containing TC12TMA. (d) Particles containing polymerized TC12TMA.

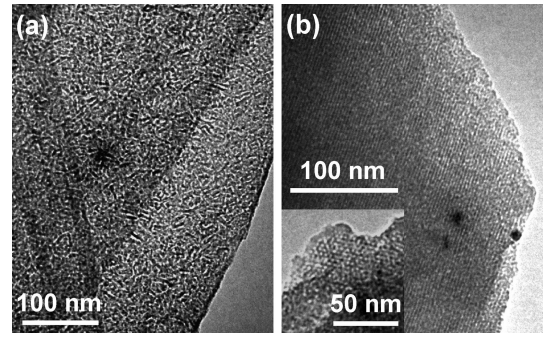

Figure 3. TEM images of calcined mesoporous silica particles. (a) Particles prepared with TC10TMA. (b) Particles prepared with TC12TMA. The image is recorded along the [110] zone axis. The inset is a image recorded along the [001] zone axis.

We recorded SAXRD patterns on the dried, as-prepared composite particles made with the two thiophene-containing surfactants (Figure 2a,c). The SAXRD pattern recorded on the spherical particles prepared with TC10TMA exhibits a broad diffraction peak centered around $2\theta = 2.2°$ ($d = 4.0$ nm), while that recorded on the particles prepared with TC12TMA shows a sharp diffraction peak centered at $2\theta = 2.42°$ ($d = 3.65$ nm). The appearance of a sharp diffraction peak suggests that the mesostructure of the particles with curved morphologies is better ordered than that of the spherical particles.

TEM imaging was further performed to characterize the internal mesostructures of the products synthesized with TC10TMA and TC12TMA. In order to increase the contrast between the pore channels and silica pore walls for clear observation of the mesostructure under TEM imaging, the products were calcined and slightly ground into small pieces. Parts a and b of Figure 3 show typical TEM images of the calcined products made with TC10TMA and TC12TMA, respectively. Wormlike pore channels are observed in the spherical particles made with TC10TMA, while parallel pore channels are clearly seen in the particles with curved morphologies and made with TC12TMA. The parallel pore channels are hexagonally ordered, as revealed by TEM

imaging under appropriate orientations (Figure 3b, inset). Such hexagonally ordered parallel pore channels are typical of a two-dimensional hexagonal mesostructure.

The different morphologies exhibited by the products synthesized with the two thiophene-containing surfactants, we believe, result from the interplay between the internal packing energy of organic and inorganic components and the external solid–liquid interfacial energy between the synthesis products and liquid growth solutions. The TC12TMA-directed particles have curved morphologies, and their external surface area is therefore larger than that of the TC10TMA-directed spherical particles if their volumes are assumed to be equal. The increase in the external interfacial energy must be counterbalanced by the decrease in the internal packing energy in order to minimize the total energy for the TC12TMA-directed particles. This is in agreement with the observation from the XRD and TEM characterizations that the TC12TMA-directed mesostructure is better ordered than the TC10TMA-directed one. The pore channels in the TC12TMA-directed mesostructure tend to wind inside in order to increase the interaction between organic and inorganic components. As a result, the external surfaces of the TC12TMA-directed particles follow the winding pore channels to result in the curved morphologies. In addition, the *d* spacing of the TC12TMA-directed particles is smaller than that of the TC10TMA-directed particles even though the hydrophobic tail of TC12TMA is longer than that of TC10TMA. This can also be attributed to the better ordered mesostructure directed by TC12TMA, where the dense packing of organic and inorganic components leads to a smaller *d* spacing. The better ordering observed in the TC12TMA-directed mesostructure is essentially due to the larger hydrophobic interaction between the longer tails, as supported by the previous estimation that the standard free energy of micellization becomes more negative as the hydrophobic tail of alkyltrimethylammonium bromide surfactant gets longer.[22]

The thiophene groups are packed together in the central regions of the pore channels of the TC10TMA- and TC12TMA-directed mesostructured silica particles. The dense packing of the thiophene groups permits them to be polymerized within the pore channels to form mesostructured polythiophene–silica composite particles (Scheme 2). In situ thiophene polymerization was carried out by mixing the composite particles with anhydrous $FeCl_3$, a thiophene polymerization oxidant,[23] in chloroform and stirring the mixture at room temperature for 48 h. SEM imaging shows that the morphologies of the composite particles are well-preserved after polymerization (Figure 4). The surfaces of the mesostructured spherical polyTC10TMA–silica and gyroidal polyTC12TMA–silica composite particles remain to be smooth. Moreover, the SAXRD patterns (Figure 2b,d) recorded on the composite particles show the preservation of the diffraction peaks after polymerization. These results indicate that the silica mesostructure is robust enough to withstand the polymerization process and confine the polythiophene chains inside the silica pore channels. The diameter of these silica pore channels is estimated to be between 2 and 3 nm from the TEM and SAXRD characterizations and the typical pore wall thickness of mesostructured silica materials synthesized using alkyltrimethylammonium surfactants under acidic conditions.[11,15–17]

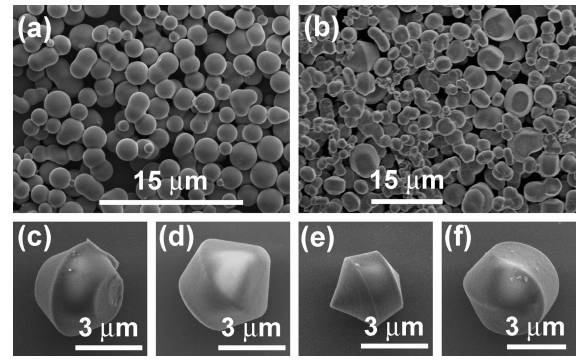

Figure 4. SEM images of mesostructured polythiophene–silica composite particles. (a) Spherical particles containing polymerized TC10TMA. (b) Particles that have curved morphologies and contain polymerized TC12TMA. (c–f) Zoomed-in images of individual particles that have different shapes and contain polymerized TC12TMA.

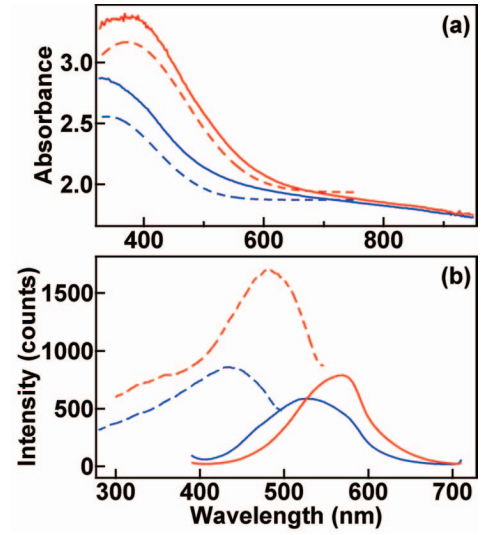

Figure 5. Optical properties of mesostructured polythiophene–silica composite particles. (a) UV–vis absorption spectra of mesostructured polyTC10TMA–silica (blue lines) and polyTC12TMA–silica (red lines) composite particles. The dashed lines are the absorption peaks obtained by fitting the absorption spectra with a combination of a Gaussian peak and a linear background. (b) Fluorescence emission (solid lines) and fluorescence–excitation (dashed lines) spectra of mesostructured polyTC10TMA–silica (blue lines) and polyTC12TMA–silica (red lines) composite particles. The excitation is at 350 nm, and the monitoring wavelengths of the fluorescence–excitation spectra are 529 and 569 nm for polyTC10TMA–silica and polyTC12TMA–silica composite particles, respectively.

In situ polymerization induces a color change from white to reddish brown for both composite particle samples, suggesting the formation of conjugated polythiophene chains within the nanoscale silica pore channels. UV–vis absorption and fluorescence spectra were measured to characterize the optical properties of both mesostructured polythiophene–silica composite particle samples. Figure 5a shows the absorption spectra of the particles dispersed in aqueous solutions. Because of the presence of an increasing back-

(22) Gao, J. X.; Bender, C. M.; Murphy, C. J. *Langmuir* **2003**, *19*, 9065.
(23) (a) Pomerantz, M.; Tseng, J. J.; Zhu, H.; Sproull, S. J.; Reynolds, J. R.; Uitz, R.; Arnott, H. J. *Synth. Met.* **1991**, *41–43*, 825. (b) Niemi, V. M.; Knuuttila, P.; Österholm, J.-E.; Korvola, J. *Polymer* **1992**, *33*, 1559.

ground toward the shorter wavelength that results from the scattering off the micrometer-sized composite particles, we fitted the absorption spectra using a combination of a Gaussian peak and a linear background. The resulting Gaussian peaks for the particles containing polyTC10TMA and polyTC12TMA are centered at 339 and 372 nm, respectively. Figure 5b shows the fluorescence (solid lines) and fluorescence–excitation (dashed lines) spectra of the two composite particle samples. The polyTC10TMA–silica and polyTC12TMA–silica composite particles exhibit fluorescence peaks centered around 529 and 569 nm, respectively. Their fluorescence–excitation spectra, monitored at their respective fluorescence peak wavelengths, show peaks around 435 and 481 nm, respectively. It is clearly seen that the maximum absorption wavelength, the fluorescence peak wavelength, and the fluorescence–excitation peak wavelength of the polyTC12TMA–silica composite particles are all longer than the corresponding wavelengths of the polyTC10TMA–silica composite particles.

The maximum absorption and fluorescence emission wavelengths of conjugated polymers are determined by their effective conjugation lengths. The effective conjugation lengths of the polyTC10TMA and polyTC12TMA in the mesostructured silica particles can be estimated according to their absorption and fluorescence emission wavelengths. Previous theoretical calculations and experimental measurements have shown that the maximum absorption and fluorescence emission energies of unsubstituted and substituted oligothiophenes increase nearly linearly with the inverse of the number of thiophene rings.[24] From the maximum absorption wavelengths, the effective conjugation lengths of the polyTC10TMA and polyTC12TMA are estimated to be 1.3 and 1.7 nm, corresponding to 3 and 4 substituted thiophene rings, respectively. From the fluorescence emission wavelengths, the effective conjugation lengths are estimated to be 2.9 and 8.4 nm, corresponding to 7 and 20 substituted thiophene rings, respectively. The fluorescence emission energy of the polyTC12TMA is close to the polythiophene limit of an infinite number of thiophene rings, suggesting that the effective conjugation length of the polyTC12TMA is even larger. The larger effective conjugation lengths of the polyTC12TMA compared to those of the polyTC10TMA in their respective mesostructured silica composite particles can be ascribed to the difference in their mesostructures because the conjugated polythiophene chains are confined within the nanoscale silica pore channels. The pore channels in the polyTC10TMA–silica composite particles are wormlike, with a large number of sharp bends and twists along the pore channels (Figure 3a). In contrast, the polyTC12TMA–silica composite particles possess a two-dimensional hexagonal mesostructure. The pore channels are straight, and their lengths are up to several hundred nanometers (Figure 3b). For conjugated polymers, it has been known that bends and twists on a conjugated polymer chain generally reduce the effective conjugation length of the polymer chain.[25] The longer conjugated segments will have smaller $\pi \rightarrow \pi^*$ energy gaps while the energy gaps of shorter conjugated segments will be larger. The wormlike mesostructure of the polyTC10TMA–silica composite particles leads to a shorter average effective conjugation length because of the presence of a large number of bends and twists along the pore channels, while the two-dimensional hexagonal mesostructure of the polyTC12TMA–silica composite particles results in a longer average effective conjugation length because of the long and straight pore channels. As a result, the maximum absorption and fluorescence emission energies of the polyTC10TMA–silica particles are larger than those of the polyTC12TMA–silica particles. There are other factors that can also affect the effective conjugation lengths because the lengths of a considerable number of the straight pore channels between neighboring bends/twists in the polyTC10TMA–silica composite particles are up to ~10 nm (Figure 3a). One possible factor is that the diffusion of the polymerization oxidant, $FeCl_3$, into the interior of the polyTC12TMA–silica particles through the straight pore channels is easier than that into the interior of the polyTC10TMA–slica particles through the wormlike pore channels. The easier diffusion of $FeCl_3$ increases the extent of thiophene polymerization. Another possible factor is that the longer tail of TC12TMA is more flexible and accommodating and therefore leads to larger effective conjugation lengths, as has been demonstrated previously in the polymerization of thiophene monomers substituted with alkyl chains of different lengths at the third position of the thiophene ring.[26]

The fluorescence emission peak energies for both types of composite particles are highly Stokes-shifted compared to the fluorescence–excitation peak energies because excitons on higher energy segments can undergo rapid energy transfer to lower energy segments, so that nearly all the fluorescence emission comes from lower energy segments of longer conjugation lengths. In addition, the absorption peak energies for both types of composite particles are largely blue-shifted relative to both fluorescence emission and fluorescence–excitation peak energies. This suggests that excitons formed by the excitation at the absorption peak energies are not able to transfer to the lowest energy segments, which is probably due to that the polythiophene chains in the composite particles are confined in the nanoscale silica pore channels.

The mesostructured polythiophene–silica composite particles exhibit bright, photostable fluorescence emission. The integrated fluorescence intensity of the polyTC12TMA–silica composite particle dispersion solution has been compared to that measured on a dispersion solution of rhodamine 6G-containing mesostructured silica particles prepared using cetyltrimethylammonium bromide as the structure-directing agent under the conditions similar to those for the preparation of the thiophene-containing silica particles (see Figure S1 in Supporting Information). The fluorescence intensity of a polyTC12TMA–silica composite particle with a typical

(24) (a) Bäuerle, P. *Adv. Mater.* **1992**, *4*, 102. (b) Becker, R. S.; de Melo, J. S.; Maçanita, A. L.; Elisei, F. *J. Phys. Chem.* **1996**, *100*, 18683. (c) Lacroix, J. C.; Chane-Ching, K. I.; Maquère, F.; Maurel, F. *J. Am. Chem. Soc.* **2006**, *128*, 7264. (d) Gierschner, J.; Cornil, J.; Egelhaaf, H.-J. *Adv. Mater.* **2007**, *19*, 173.

(25) Schwartz, B. J. *Annu. Rev. Phys. Chem.* **2003**, *54*, 141.

(26) (a) Chen, S.-A.; Ni, J.-M. *Macromolecules* **1992**, *25*, 6081. (b) Ho, K.-S.; Bartus, J.; Levon, K.; Mao, J.; Zheng, W.-Y. *Synth. Met.* **1993**, *55–57*, 384.

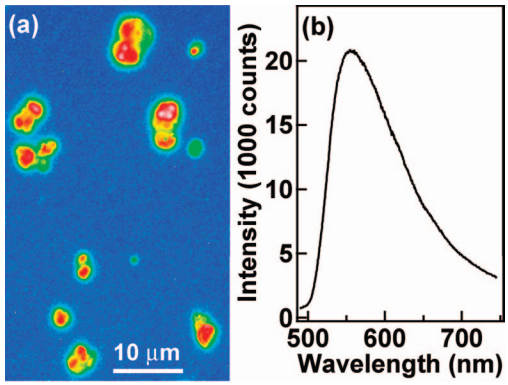

Figure 6. (a) Fluorescence image of mesostructured polyTC12TMA–silica composite particles deposited on a glass slide. (b) Representative fluorescence spectrum acquired from a single polyTC12TMA–silica particle. The asymmetric emission spectrum is due to the use of a long-pass filter to remove the excitation laser light.

diameter of 5 μm is estimated to be equivalent to that of a 5 μm diameter silica particle containing 1.8×10^8 rhodamine 6G molecules. When deposited on glass slides, the fluorescence emission from individual particles under laser light excitation at 457 nm can readily be seen by eye through an objective. Figure 6a shows a representative fluorescence image of the mesostructured polyTC12TMA–silica composite particles deposited on a glass slide. A typical fluorescence emission spectrum taken from a single particle is shown in Figure 6b. The fluorescence emission peak energy measured on individual polyTC12TMA–silica composite particles is close to that measured on the aqueous dispersion of the particles. The fluorescence intensities of individual polyTC12TMA–silica composite particles have been monitored as a function of time under continuous laser illumination (see Figure S2 in Supporting Information). They drop to 10−40% of the initial fluorescence intensities after 1 h of laser illumination. In comparison, single organic dye molecules are known to survive for only several minutes under typical imaging conditions.[27] The fluorescent polythiophene–silica composite particles could therefore be of particular use in a number of applications, including tagging, tracing, and labeling.[19,28,29]

Conclusions

Two cationic surfactants with a thiophene group at one end of a carbon chain and a trimethylammonium headgroup at the other end of the carbon chain have been synthesized and used as structure-directing agents to direct the formation of mesostructured silica particles. The synthesis using the surfactant with a 10-carbon chain in between the thiophene group and the trimethylammonium headgroup under acidic conditions produces micrometer-sized spherical particles with a wormlike mesostructure. The synthesis using the surfactant with a 12-carbon chain yields micrometer-sized particles that have curved morphologies and possess a two-dimensional hexagonal mesostructure. The dense packing of thiophene groups in the central region of the nanoscale silica pore channels allows them to be in situ polymerized to form mesostructured polythiophene–silica composite particles. These composite particles emit bright and stable fluorescence. Moreover, the absorption and fluorescence emission peaks of the mesostructured composite particles with curved morphologies are red-shifted relative to those of the spherical particles because the average effective conjugation length of the polythiophene chains confined in the silica pore channels of the hexagonal mesostructure is longer than that in the pore channels of the wormlike mesostructure. We believe that our demonstrated strategy of confining conjugated polymers within nanoscale inorganic pore channels through self-assembly can be applied to the preparation of a wide range of functional mesostructured composite materials composed of different organic polymers and inorganic frameworks and with different morphologies, including fibers and thin films.

Acknowledgment. This work was supported by a RGC CERG grant (Ref. No.: 403006, Project Code: 2160293).

Supporting Information Available: Fluorescence spectra of the dispersion solutions of the polyTC12TMA- and rhodamine 6G-containing mesostructured silica particles measured under the same excitation conditions and fluorescence intensity changes of individual polyTC12TMA–silica particles as a function of the laser illumination time. This information is available free of charge via the Internet at http://pubs.acs.org.

CM7020005

(27) Fraser, S. E. *Nat. Biotechnol.* **2003**, *21*, 1272.
(28) Sokolov, I.; Kievsky, Y. Y.; Kaszpurenko, J. M. *Small* **2007**, *3*, 419.
(29) (a) Han, M. Y.; Gao, X. H.; Su, J. Z.; Nie, S. M. *Nat. Biotechnol.* **2001**, *19*, 631. (b) Edwards, B. S.; Oprea, T.; Prossnitz, E. R.; Sklar, L. A. *Curr. Opin. Chem. Biol.* **2004**, *8*, 392. (c) Zhao, X. J.; Hilliard, L. R.; Mechery, S. J.; Wang, Y. P.; Bagwe, R. P.; Jin, S. G.; Tan, W. H. *Proc. Natl. Acad. Sci. U.S.A.* **2004**, *101*, 15027. (d) Wang, L.; Yang, C. Y.; Tan, W. H. *Nano Lett.* **2005**, *5*, 37.